Molecular to Atomic Phase Transition in Hydrogen under High Pressure

Jeremy McMinis, Raymond C. Clay, III, Donghwa Lee, and Miguel A. Morales

Phys. Rev. Lett. **114**, 105305 — Published 13 March 2015

DOI: 10.1103/PhysRevLett.114.105305

The molecular to atomic phase transition in high pressure hydrogen

Jeremy McMinis,[1] Raymond Clay III,[2,1] Donghwa Lee,[1] and Miguel A. Morales[1,*]

[1]*Lawrence Livermore National Laboratory, Livermore, California USA 94550*

[2]*University of Illinois, Urbana, Illinois USA 61821*

(Dated: February 2, 2015)

Abstract

The metallization of high pressure hydrogen, together with the associated molecular-to-atomic transition, is one of the most important problems in the field of high pressure physics. It is also currently a matter of intense debate due to the existence of conflicting experimental reports on the observation of metallic hydrogen on a diamond anvil cell. Theoretical calculations have typically relied on a mean-field description of electronic correlation through density functional theory, a theory with well-known limitations in the description of metal-insulator transitions. In fact the predictions of the pressure driven dissociation of molecules in high pressure hydrogen by density functional theory is strongly affected by the chosen exchange-correlation functional. In this article we use quantum Monte Carlo calculations to study the molecular-to-atomic transition in hydrogen. We obtain a transition pressure of 447(3) GPa, in excellent agreement with the best experimental estimate of the transition, 450 GPa, based on an extrapolation to zero band gap from experimental measurements. Additionally, we find that $C2/c$ is stable almost up to the molecular-to-atomic transition, in contrast to previous DFT and DFT+QMC studies which predict large stability regimes for intermediary molecular phases.

Hydrogen is the simplest and most abundant atom in the universe, yet its behavior at high pressures is one of the most puzzling [8, 9]. Being the lightest element in the periodic table, its strong quantum nature at low temperatures and subtle electronic structure lead to very interesting physics which include: multiple orientationally-ordered molecular phases [2, 4, 10], a re-entrant melting line [11–14], a liquid-liquid phase transition [15–17], and a metal-insulator transition accompanied with the possibility of exotic physics including superconductivity [18] and a zero-temperature liquid [19]. Describing the physics of these processes and its equation of state with quantitative accuracy is of critical importance to many areas of physics including astrophysics, planetary science, material science, and inertial confinement fusion research.

Because hydrogen is highly reactive and diffusive, attempts to experimentally synthesize metallic hydrogen in diamond-anvil cell experiments are difficult, and sometimes produce conflicting predictions. It has been claimed that metallic hydrogen may have been observed very recently by Eremets, *et al* [1]. While these findings have yet to be confirmed and are considered highly controversial, they resulted in a significant increase in attention on this regime of the phase diagram over the last several years [3, 20–25]. As a result, a new high pressure molecular phase was discovered at room temperature, phase IV [2, 26, 27], and the phase boundaries between the various molecular phases have been further clarified [4].

To date, the best experimental estimate of the location of the metal-insulator transition at 0K is at approximately 450 GPa [7]. This estimate was produced by extrapolation of the band gap to zero as a function of pressure and assumes that hydrogen remains in phase III up to the transition. Because of hydrogen's small x-ray scattering cross-section a definitive determination of whether it remains in this phase through the observed range is difficult. Determining whether it remains in phase III beyond the experimentally accessible regime must be done using *ab initio* methods. We do so by providing an accurate equation of state to confirm the validity of Loubeyre *et al.*'s extrapolations.

For a theoretical method to be predictive in this regime, both electronic structure (e.g. electronic correlation) and nuclear quantum effects (which are very strong) must be treated accurately [5, 6]. Because of its established unmatched accuracy in bulk low Z systems[16, 36–38] and its ability to capture many-body electronic correlation[36, 38–41], we used fixed-node Diffusion Monte Carlo to directly estimate ground-state energies, pressures, enthalpies, and geometries of the atomic phases. To treat nuclear quantum effects,

we employ the quasi-harmonic approximation. Here, as well as in geometry optimization for the molecular phases, we used DFT instead of DMC for cost reasons. Unlike previous QMC/DFT studies however, we heavily use DMC to benchmark the effect of DFT approximation on properties like vibrational frequencies and ground-state enthalpies, which allows us to somewhat mitigate this approximation by choosing the most accurate functionals for our applications and estimating the errors in doing so.

Our results show that the molecular-to-atomic phase transition occurs around 447(3) GPa. Though we formally observe this transition to be from $C2/c$ →Cmca–12→Cs–IV, we find a small regime of stability for the $Cmca-12$ phase of 24(4) GPa, in stark contrast to previous DFT and QMC+DFT studies which unambiguously predict one or more intermediary molecular phases between $C2/c$ →Cs–IV. Interestingly, a vanishingly small or entirely absent intermediary phase between $C2/c$ and $Cs–IV$ is in good agreement with the assumption a single molecular phase in Loubeyre *et al*'s extrapolation.

All QMC calculations were performed with the Quantum Monte Carlo Package (QMCPACK) [45]. We used the full Coulomb potential and a Slater-Jastrow trial wave function. The Jastrow consists of one and two body B-spline terms. We optimize all variational parameters using the linear method [46]. The single particle orbitals are generated using the Quantum Espresso density functional theory code [47]. We use a PBE exchange correlation functional and a norm-conserving pseudopotential with a cutoff radius of 0.5 bohr. To control for finite-size effects, we used twist-averaged boundary conditions [48] in all DMC calculations, with a 24^3 Monkhorst-Pack K-point grid for the 4 atom unit cell in the atomic phase and 6^3 Monkhorst-Pack K-point grid for the 96 atom unit cell in the molecular phase. Simulation cells of various sizes were used to extrapolate the energies to the thermodynamic limit [44]. Pressures were computed using the extrapolated virial estimator, as well as by differentiation of the energy.

DFT calculations were performed with the Vienna Ab-Initio Simulation Package (*VASP*) [49, 50]. We used the projector augmented wave (PAW) representation of *VASP*, with a PAW constructed with PBE from their most recent release. Geometry optimization and ground-state calculations were performed for all structures on unit cells containing between 4 and 48 atoms, using plane-wave cutoffs of 1000eV and 1500 eV for the geometry optimization and ground-state calculations respectively. Though different Monkhorst-Pack k-point grids were used for different structures, we ensured that energies and pressures were con-

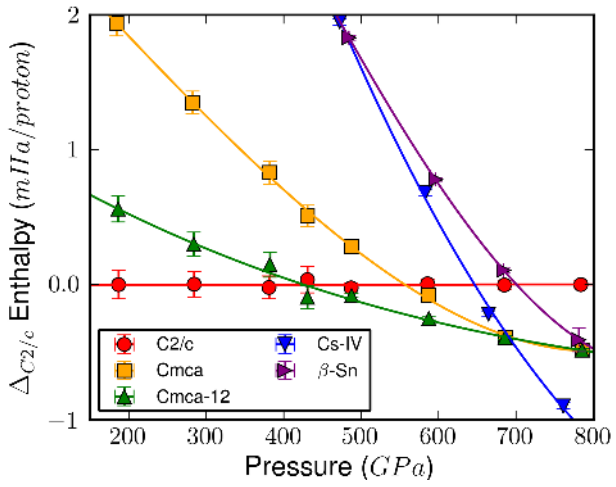

FIG. 1: Static lattice enthalpy of molecular and atomic phases relative to the molecular $C2/c$ crystal. In the absence of ZPE, the phase transition happens at 684(3) GPa.

verged. All ZPE calculations reported on this article were calculated with the *Phonopy* code (http://phonopy.sourceforge.net/) and were based on the quasi-harmonic approximation. All ZPE calculations on the molecular phases employed 728 atoms, while all calculations on the atomic phase employed 432 atoms. We carefully tested that the resulting ZPEs were well converged by using cells with up to 2592 and 1600 atoms on the molecular and atomic phase respectively.

To compute the location of the molecular-to-atomic phase transition we start with a selection of the most important candidate structures for each phase and optimize their geometries. On the atomic side we selected the only 2 competing phases: $\beta-$tin and $Cs–IV$. We performed random structure searches with both PBE and vdW-DF DFT functionals to look for new atomic phases at pressures around 500 GPa and found no new structure that is competitive with the ones considered in this work.

Since both of these structures have only one variable parameter in their geometry, namely the c/a ratio, we directly optimized their geometries with DMC at several volumes in the pressure range $450-800$ GPa. On the molecular side we selected the three candidate phases: $C2/c$, $Cmca$, and $Cmca$–12. Two of these phases, $C2/c$ and $Cmca$–12, were discovered in the pioneering work on C. Pickard and R. Needs [51] using Ab-Initio Random Structure Searching with DFT, we refer the reader to this article for a detailed description of the structures. These phases are three of the leading candidate structures for phase III accord-

ing to DFT [22] and are the most promising alternatives close to the molecular to atomic transition according to QMC calculations [43]. The large number of degrees of freedom in these structures prevent us from a direct optimization of the geometry with DMC. Instead, we optimized the geometries and atomic positions at selected pressures using three different DFT exchange correlation functionals (vdW-DF, vdW-DF2, PBE) and performed a detailed comparison of the resulting energies. This not only allows us to choose the best structure out of three candidates with the lowest QMC enthalpy, but allows us to roughly establish how the quality of optimized structures depends on the choice of density functional. For all structures and pressures considered in this work, the vdW-DF functional provided the best ground state geometries. The difference in enthalpy between structures optimized at similar pressures with different functionals was found to be as large as 0.4 $mHa/atom$, with the structures produced by PBE always consistently worse than those generated by either vdW-DF or vdW-DF2. We refer the reader to the work of Clay, *et al.* [43], for a detailed analysis of the quality of various density functionals on the molecular phase, benchmarked against DMC.

Figure 1 shows the enthalpy of the lattice with clamped protons (without zero-point energy) for all the structures considered in this work between $200 - 800$ GPa. Our QMC calculations show that the molecular-to-atomic transition in the absence of ZPE occurs at 685(6) GPa, following the sequence $C2/c$ →Cmca–12→Cs–IV

In Figure 2, we show the DFT clamped-nuclei cold-curves, produced using the following functionals: PBE, HSEsol, HSE, vdW-DF and vdW-DF2. Contrasting this with our QMC cold-curve, we note several quantitative and qualitative differences. Qualitatively, all functionals predict the stability of the $Cmca$ phase between Cmca–12→Cs–IV, which is unstable according to QMC. Quantitatively, the onset of the molecular-to-atomic transition varies wildly based on functional choice, differing from QMC and eachother. According to PBE, the transition occurs around 500 GPa between $Cmca$ and $Cs–IV$ structures, which is around 185 GPa lower than the QMC estimate. Both vdW functionals predict much higher transitions than QMC, by almost 100 GPa and 300 GPa for the vdW-DF and vdW-DF2 respectively. This amounts to an uncertainty of about 500 GPa.

The results for the static lattice show the strong dependence of the molecular dissociation pressure on the functional's relative accuracy in the metallic and molecular states. However, no prediction can be made without a careful treatment of the ZPE. As mentioned previously,

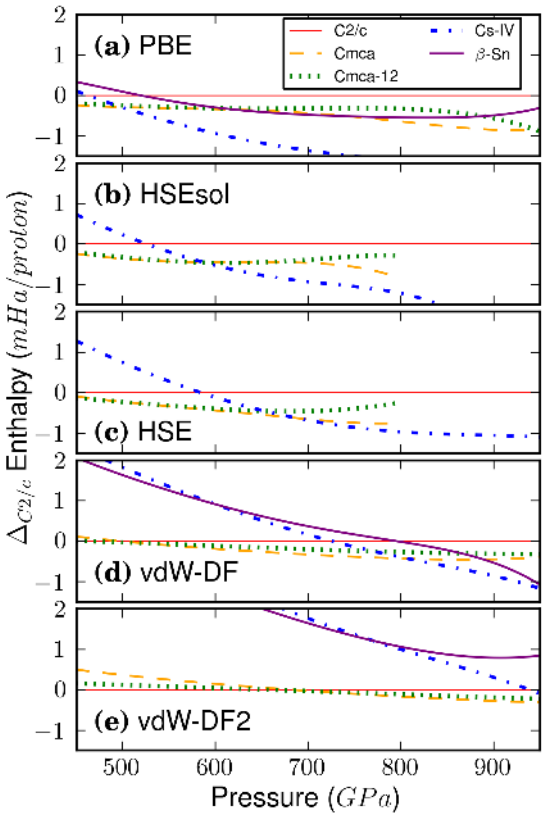

FIG. 2: DFT electronic structure contribution to Enthalpy for five functionals: (a) PBE, (b) HSEsol, (c) HSE, (d) vdW-DF and (e) vdW-DF2.

an accurate treatment of the ZPE with DMC is beyond the current capabilities of the method. Instead, we must resort to a more approximate treatment within DFT. To make the task more complicated, the ZPE predicted by DFT is quite dependent on the functional used on the molecular phase. As described in the supplementary material [44], the variations of the magnitude of the ZPE component with DFT functional on the atomic side is on the order of 0.2 $mHa/atom$ and basically independent of structure. On the molecular side, the variation is bigger than 1.0 $mHa/atom$ and can be as large as 2.0 $mHa/atom$.

In contrast to the atomic phase, intramolecular vibrations provide the dominant contribution to the ZPE in the molecular phase. There is a strong variation in the description of the molecular bond and the corresponding intramolecular potential between the different DFT functionals [43, 44]. This variation leads to the observed discrepancy on the magnitude of the ZPE in each phase. Using correlated sampling combined with reptation quantum Monte Carlo we studied the dependence of the energy of the crystal with molecular bond length.

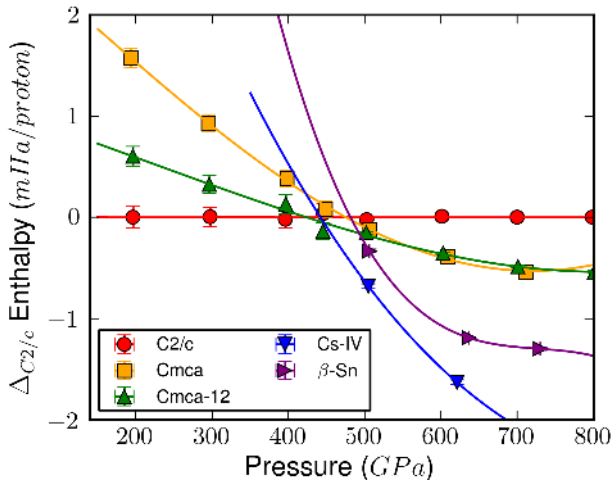

FIG. 3: Enthalpy of molecular and atomic phases relative to the molecular $C2/c$ crystal. We find a phase transition from molecular-to-atomic hydrogen at 439(3) GPa.

This allows us to optimize the bond lengths with DMC and compare them against DFT results, as well as to measure the curvature of the molecular potential at the equilibrium bond length, which is directly related to the vibrational frequency of the molecule and to the magnitude of the ZPE. We find a direct correlation between the molecular bond length, as predicted by DFT, and the magnitude of the corresponding ZPE (see Supplementary Material). The vdW-DF functional produces the best overall agreement in all aspects of the molecular bond in hydrogen: the magnitude of the bond length (accurate to $\approx 1\%$), pressure dependence, and the curvature of the intramolecular potential. In contrast, PBE systematically underestimates the bond-length (by 5%) and ZPE, whereas vdW-DF2 overestimates the bond-lengths (by up to $\approx 4\%$) and ZPE. We conclude that vdW-DF provides the most accurate estimate of the ZPE in these molecular phases, due to its good agreement with QMC, and choose it to provide the ZPE contribution we use for our QMC results. While HSE also offers a reasonable description of the structural and vibrational properties of the solid, we have not attempted to calculate the transition pressure with ZPE from this functional.

Our main result, the total enthalpy (including QMC electronic contribution and DFT quasi-harmonic ZPE) of all the structures considered in this work, is shown in Figure 3. We find the transition from molecular $C2/c$ to the atomic Cs–IV phases to follows the progression $C2/c$ →Cmca–12→Cs–IV, with transition pressures between $C2/c$ →Cmca–12

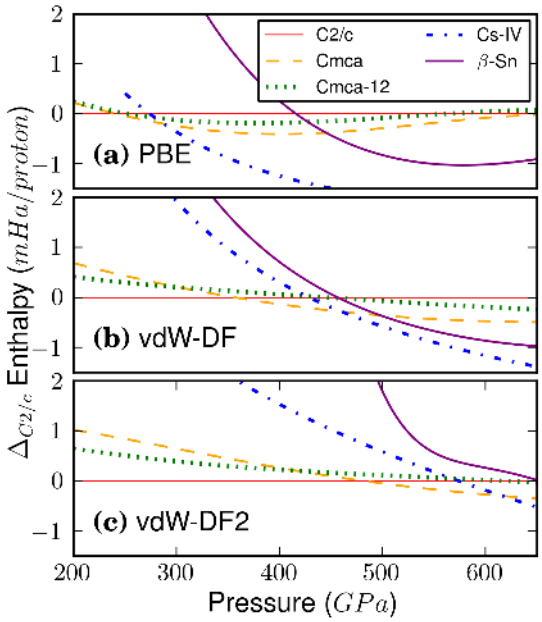

FIG. 4: Enthalpy vs Pressure for three DFT exchange correlation functionals: (a) PBE, (b) vdW-DF and (c) vdW-DF2. Zero-point energy shifts the transition down a few hundred GPa for each functional but the *Cmca* phase is still stable, and immediately precedes the atomic Cs–IV phase.

and Cmca–12→Cs–IV occurring at 424(3) and 447(3) GPa respectively. Note that the regime of stability for the *Cmca*–12 phase is actually quite small–about 24(4) GPa. Though this is statistically significant, the enthalpy differences responsible for the stability of the *Cmca*–12 phase are so small that that the stability of *Cmca*–12 will very sensitive to higher order effects, such as anharmonic corrections to the ZPE. For this reason, in the future we suggest investigating the direct molecular-to-atomic transition $C2/c$ →Cs–IV at a higher level of theory, which would occur at 442(3) GPa in the absence of Cmca–12 at the quasi-harmonic level.

For comparison, we include the corresponding ZPE corrected DFT total enthalpy plots for the PBE, vdW-DF, and vdW-DF2 functionals in Figure 4. ZPE contributions shift the phase transition downwards between 200 for PBE to $400GPa$ for vdW-DF2 and reduces but does not eliminate the region of stability for the *Cmca* phase. The resulting molecular disassociation transition ranges from 288 for PBE to 617 GPa for vdW-DF2 with only the vdW-DF function close to the QMC result at 461 GPa.

According to self-consistent GW calculations on static lattices, the $C2/c$ molecular phase

has a finite band gap at the transition pressure (See the supplementary material [44] for additional details). In contrast, Cmca–12 and Cs–IV are expected to be metallic. Thus, our current work seems to imply that at the quasi-harmonic level, the insulator-to-metal transition would coincide with the $C2/c \rightarrow$Cmca–12 molecular transition. Nuclear quantum fluctuations have been shown to have a strong influence on the band gap of solid hydrogen [6] and a definite prediction of the pressure where the band gap closes goes beyond the scope of this article.

Interestingly, our results disagree with previous QMC studies on the structural transitions in solid hydrogen by Azadi *et al.* [54, 55]. We attribute this to several subtle approximations in their work which has been shown in this and other works to be inadequate. Their use of the LDA based Kwee-Zhang-Krakauer finite-size correction scheme introduces non-consistent errors in enthalpy differences of up to $\pm 0.5 mHa$, depending on the structures and pressure. Secondly, they used PBE to optimize their zero temperature configurations, which from Clay *et al.* [43] is shown to yield higher enthalpy structures than vdW-DF. It is worth noting that according to PBE at low temperatures atomic hydrogen is stable at pressures above 288 GPa, which is in complete disagreement with experimental observations. PBE systematically fails to accurately describe hydrogen close to the dissociation regime. On the one hand, it provides a very poor description of the intramolecular interaction by greatly overestimating the bond length and underestimating the curvature of the potential (and hence the vibrational frequency). On the other hand, it strongly reduces the energy of the atomic phases relative to the molecular ones, leading to very low transition pressures.

The promise of observing metallic hydrogen at low temperature is within close reach of current experimental techniques. Our calculation brings current *ab initio* predictions for the molecular-to-atomic phase transition into much better alignment with experiment. First, we find the molecular-to-atomic phase transition occurs around 447(3) GPa, which agrees with previous experimental results and Loubeyre *et al.*'s extrapolation. Second, we find that in contrast to previous DFT and QMC+DFT studies, which predict undeniably stable secondary molecular phases, the C2/c phase is robust and stable almost all the way to the molecular-to-atomic transition. At finite temperature the phase diagram could be more complicated due to the existence of additional stable phases [22] and more complicated physical processes including proton transfer [23].

This work was supported by the U.S. Department of Energy at the Lawrence Livermore

National Laboratory under Contract DE-AC52-07NA27344 and by LDRD Grant No. 13-LW-004. Computer resources have been provided by Lawrence Livermore National Laboratory through the 7th Institutional Unclassified Computing Grand Challenge program.

* Electronic address: moralessilva2@llnl.gov

[1] Eremets, M. & Troyan, I. Conductive dense hydrogen. *Nature materials* **10**, 927–931 (2011).

[2] Howie, R. T., Guillaume, C. L., Scheler, T., Goncharov, A. F. & Gregoryanz, E. Mixed molecular and atomic phase of dense hydrogen. *Physical Review Letters* **108**, 125501 (2012).

[3] C.S. Zha, Z. Liu, R. J. Hemley, *Phys. Rev. Lett.* **108**, 146402 (2012).

[4] Zha, C.-s., Liu, Z., Ahart, M., Boehler, R. & Hemley, R. J. High-pressure measurements of hydrogen phase iv using synchrotron infrared spectroscopy. *Phys. Rev. Lett.* **110**, 217402 (2013).

[5] Morales, M. A., McMahon, J. M., Pierleoni, C. & Ceperley, D. M. Nuclear Quantum Effects and Nonlocal Exchange-Correlation Functionals Applied to Liquid Hydrogen at High Pressure. *Physical Review Letters* **110**, 065702 (2013). URL http://link.aps.org/doi/10.1103/PhysRevLett.110.065702.

[6] Morales, M. A., McMahon, J. M., Pierleoni, C. & Ceperley, D. M. Towards a predictive first-principles description of solid molecular hydrogen with density functional theory. *Physical Review B* **87**, 184107 (2013).

[7] Loubeyre, P., Occelli, F. & LeToullec, R. Optical studies of solid hydrogen to 320 GPa and evidence for black hydrogen. *Nature* **416**, 613–7 (2002). URL http://www.ncbi.nlm.nih.gov/pubmed/11948345.

[8] Chang, K. The big squeeze. *The New York Times* (2013). URL http://www.nytimes.com/2013/12/17/science/the-big-squeeze.html?pagewanted=all&_r=0.

[9] McMahon, J. M., Morales, M. A., Pierleoni, C. & Ceperley, D. M. The properties of hydrogen and helium under extreme conditions. *Reviews of Modern Physics* **84**, 1607 (2012).

[10] Mao, H.-k. & Hemley, R. J. Ultrahigh-pressure transitions in solid hydrogen. *Rev. Mod. Phys.* **66**, 671–692 (1994).

[11] Bonev, S. A., Schwegler, E., Ogitsu, T. & Galli, G. A quantum fluid of metallic hydrogen suggested by first-principles calculations. *Nature* **431**, 669–72 (2004). URL http://www.

ncbi.nlm.nih.gov/pubmed/15470423.

[12] Deemyad, S. & Silvera, I. Melting Line of Hydrogen at High Pressures. *Physical Review Letters* **100**, 155701 (2008). URL http://link.aps.org/doi/10.1103/PhysRevLett.100.155701.

[13] Eremets, M. I. & Trojan, I. A. Evidence of maximum in the melting curve of hydrogen at megabar pressures. *JETP Letters* **89**, 174–179 (2009). URL http://link.springer.com/10.1134/S0021364009040031.

[14] Subramanian, N., Goncharov, A. F., Struzhkin, V. V., Somayazulu, M. & Hemley, R. J. Bonding changes in hot fluid hydrogen at megabar pressures. *Proceedings of the National Academy of Sciences of the United States of America* **108**, 6014–9 (2011). URL http://www.pubmedcentral.nih.gov/articlerender.fcgi?artid=3076824\&tool=pmcentrez\&rendertype=abstracthttp://www.pnas.org/content/108/15/6014.short.

[15] Scandolo, S. Liquid-liquid phase transition in compressed hydrogen from first-principles simulations. *Proceedings of the National Academy of Sciences of the United States of America* **100**, 3051–3 (2003). URL http://www.pubmedcentral.nih.gov/articlerender.fcgi?artid=152244\&tool=pmcentrez\&rendertype=abstract.

[16] Morales, M. A., Pierleoni, C., Schwegler, E. & Ceperley, D. M. Evidence for a first-order liquid-liquid transition in high-pressure hydrogen from ab initio simulations. *Proceedings of the National Academy of Sciences of the United States of America* **107**, 12799–803 (2010). URL http://www.pubmedcentral.nih.gov/articlerender.fcgi?artid=2919906\&tool=pmcentrez\&rendertype=abstract.

[17] Dzyabura, V., Zaghoo, M. & Silvera, I. F. Evidence of a liquidliquid phase transition in hot dense hydrogen. *Proceedings of the National Academy of Sciences* **110**, 8040–8044 (2013). URL http://www.pnas.org/content/110/20/8040.abstract. http://www.pnas.org/content/110/20/8040.full.pdf+html.

[18] Babaev, E., Sudbø, A. & Ashcroft, N. W. A superconductor to superfluid phase transition in liquid metallic hydrogen. *Nature* **431**, 666–8 (2004). URL http://www.ncbi.nlm.nih.gov/pubmed/15470422.

[19] Chen, J. *et al.* Quantum simulation of low-temperature metallic liquid hydrogen. *Nat Commun* **4** (2013).

[20] A. F. Goncharov, J. S. Tse, H. Wang, J. Yang, V. V. Struzhkin, R. T. Howie, and E. Gregoryanz, *Phys. Rev. B* **87**, 024101 (2013).

[21] A. F. Goncharov, R. T. Howie, and E. Gregoryanz, *Low Temp. Phys.* **39**, 402 (2013).

[22] H. Liu, L. Zhu, W. Cui, and Y. Ma, *J. Chem. Phys.* **137**, 074501 (2012).

[23] H. Liu and Y. Ma, *Phys. Rev. Lett.* **110**, 025903 (2013).

[24] I. I. Naumov, R. E. Cohen, R. J. Hemley, *Phys. Rev. B* **88**, 045125 (2013).

[25] R. E. Cohen, I. I. Naumov, R. J. Hemley, *PNAS* **110**, 13757-13762 (2013).

[26] P. Loubeyre, F. Occelli, P. Dumas, *Phys. Rev. B* **87**, 134101 (2013).

[27] R. T. Howie, T. Scheler, C. L. Guillaume, and E. Gregoryanz, *Phys. Rev. B* **86**, 214104 (2012).

[28] Perdew, J. P., Burke, K. & Ernzerhof, M. Generalized gradient approximation made simple. *Physical review letters* **77**, 3865 (1996).

[29] J. Heyd, G.E. Scuseria, M. Ernzerhof, *J. Chem. Phys.* **118**, 8207 (2003).

[30] L. Schimka, J. Harl, G. Kresse, *J. Chem. Phys.* **134**, 024116 (2011);

[31] Dion, M., Rydberg, H., Schröder, E., Langreth, D. C. & Lundqvist, B. I. Van der waals density functional for general geometries. *Physical review letters* **92**, 246401 (2004).

[32] Thonhauser, T. *et al.* Van der waals density functional: Self-consistent potential and the nature of the van der waals bond. *Physical Review B* **76**, 125112 (2007).

[33] Román-Pérez, G. & Soler, J. M. Efficient implementation of a van der waals density functional: application to double-wall carbon nanotubes. *Physical review letters* **103**, 096102 (2009).

[34] Lee, K., Murray, É. D., Kong, L., Lundqvist, B. I. & Langreth, D. C. Higher-accuracy van der waals density functional. *Physical Review B* **82**, 081101 (2010).

[35] Klimeš, J., Bowler, D. R. & Michaelides, A. Chemical accuracy for the van der waals density functional. *Journal of Physics: Condensed Matter* **22**, 022201 (2010).

[36] Ceperley, D. M. & Alder, B. J. Ground State of the Electron Gas by a Stochastic Method. *Physical Review Letters* **45**, 566–569 (1980). URL `http://link.aps.org/doi/10.1103/PhysRevLett.45.566http://link.aps.org/doi/10.1103/PhysRevLett.56.2415`.

[37] Morales, M. A., Pierleoni, C. & Ceperley, D. M. Equation of state of metallic hydrogen from coupled electron-ion Monte Carlo simulations. *Physical Review E* **81**, 1–9 (2010). URL `http://link.aps.org/doi/10.1103/PhysRevE.81.021202`.

[38] Khairallah, S. A. & Militzer, B. First-principles studies of the metallization and the equation of state of solid helium. *Phys. Rev. Lett.* **101**, 106407 (2008). URL `http://link.aps.org/doi/10.1103/PhysRevLett.101.106407`.

[39] Santra, B.; Michaelides, A.; Fuchs, M.; Tkatchenko, A.; Filippi, C.; Scheffler, M., *J. Chem.*

Phys. **2008**, *129*, 194111.

[40] Santra, B.; Klimes, J.; Alfè, D.; Tkatchenko, A.; Slater, B.; Michaelides, A.; Car, R.; Scheffler, M., *Phys. Rev. Lett.* **2011**, *107*, 185701.

[41] Dubeck?, Mat? and Jure?ka, Petr and Derian, Ren and Hobza, Pavel and Otyepka, Michal and Mitas, Lubos, *JCTC* **9**, 4287-4292 (2013).

[42] Azadi, S. & Foulkes, W. M. C. Fate of density functional theory in the study of high-pressure solid hydrogen. *Phys. Rev. B* **88**, 014115 (2013).

[43] Clay, R. C. *et al.* Benchmark of exchange-correlation functionals for high pressure hydrogen using quantum monte carlo. *submitted to Phys. Rev. B* (2013).

[44] Supplementary material.

[45] Kim, J. *et al.* Hybrid algorithms in quantum monte carlo. *Journal of Physics: Conference Series* **402**, 012008 (2012). URL `http://stacks.iop.org/1742-6596/402/i=1/a=012008`.

[46] Umrigar, C. J., Toulouse, J., Filippi, C., Sorella, S. & Hennig, R. G. Alleviation of the Fermion-Sign Problem by Optimization of Many-Body Wave Functions. *Physical Review Letters* **98**, 110201 (2007). URL `http://link.aps.org/doi/10.1103/PhysRevLett.98.110201`.

[47] Giannozzi, P. *et al.* QUANTUM ESPRESSO: a modular and open-source software project for quantum simulations of materials. *Journal of physics. Condensed matter : an Institute of Physics journal* **21**, 395502 (2009). URL `http://www.ncbi.nlm.nih.gov/pubmed/21832390`.

[48] Lin, C., Zong, F. & Ceperley, D. Twist-averaged boundary conditions in continuum quantum monte carlo algorithms. *Physical Review E* **64**, 016702 (2001).

[49] Kresse, G. & Furthmüller, J. Efficiency of ab-initio total energy calculations for metals and semiconductors using a plane-wave basis set. *Computational Materials Science* **6**, 15–50 (1996). URL `http://linkinghub.elsevier.com/retrieve/pii/0927025696000080`.

[50] Kresse, G. & Joubert, D. From ultrasoft pseudopotentials to the projector augmented-wave method. *Physical Review B* **59**, 1758–1775 (1999). URL `http://link.aps.org/doi/10.1103/PhysRevB.59.1758`.

[51] C. J. Pickard, R. J. Needs, Nature Physics 3, 473 - 476 (2007).

[52] P.A. Whitlock, D. M. Ceperley, G.V. Chester, M.H. and Kalos, *Phys. Rev. B* **19**, 5598 (1979).

[53] J. Casulleras and J. Boronat, *Phys. Rev. B* **52**, 3654 (1995).

[54] Azadi, S. & Foulkes, W. M. C. & Kuhne, T.D Quantum Monte Carlo study of high pressure solid molecular hydrogen. *New J. Phys.* **15**, 113005 (2013).

[55] S. Azadi, B. Monserrat, W. M. C. Foulkes, and R. J. Needs *Phys. Rev. Lett.* **112**, 165501 (2014).